FULL ELECTRICAL STRATEGY CONTROL OF WIND ENERGY CONVERSION SYSTEM BASED PMSG

A. Remli, D. Aouzellag and K. Ghedamsi
Electrical Engineering Department, Faculty of Technology, A. Mira University, 06000 Bejaia, Algeria.
remliaziz@yahoo.fr

Abstract: *This paper is devoted to the study and control of high power wind energy conversion system (WECS) based on direct driven permanent magnet synchronous generator (PMSG) connected to electrical grid. So, the WECS contains a three blade horizontal wind turbine, PMSG with high number of pole and PWM (pulse width modulation) full power converter. In partial load region, the generator side converter is controlled by means of sensorless fuzzy maximum power point tracking (MPPT) algorithm. In case the WECS rated power is reached, power is limited via generator torque control, so without pitch control. Simulation results under Matlab \ Simulink® are presented in order to validate the approach.*

Key Words: *Variable speed wind turbine, PMSG, MPPT, power limitation, fuzzy logic.*

1. Introduction

In the last two decades, various wind turbine concepts and high efficiency control schemes have been developed [1- 3]. Compared to the geared drives wind turbine concepts, using squirrel cage rotor or wound rotor generators [4, 5], the direct drive concepts may be more attractive due to advantages of simplified drive train and higher overall efficiency, reliability and availability by omitting the gearbox; which causes unpleasant noise, increase the loss and cost of wind turbine system and requires regular maintenance [6]. In direct drive wind turbine system, the PMSG becomes attractive than before, because the performance of permanent magnet materials is improving and their cost is decreasing in recent years. Moreover, PMSG have compact structure with higher ratio of power to weight, high air-gap flux density, high power density and high torque capability [7, 8].

The use of PMSG in WECS allows variable and low speed operation, which is more attractive than the fixed speed systems because of the improvement in wind energy production and reduction of the flicker problem [8]. So, the wind turbine can operate at its maximum efficiency at all wind velocities.

When the WECS reaches its rated power, this latter is limited by pitch control [9-13]. However, pitch control may have a considerable effect on the dynamical behaviour of wind generator due to malfunction problems, which affect the quality of the power injected to the grid [14]). Also, driven unit of pitch control is very cumbersome and requires regular maintenance.

In partial load region, WECS is controlled by means of MPPT algorithm which maximizes the energy captured by the turbine from the wind's kinetic energy. In the literature we find several sensorless MPPT control (without wind speed sensor) for variable wind turbine generation based induction generator or PMSG [8, 15-20]. Generator speed can be obtained by speed sensor (resolver, encoder or Hall-Effect sensor). However, a sensorless speed control of the generator can be achieved by using speed estimator [8, 21]. But these aspects are not addressed in this work. However, a sensorless fuzzy logic maximum power point tracking has been used in this work.

The main objective of the paper is to demonstrate the full electrical control feasibility of WECS in order to provide a compact structure (without gearbox and without pitch mechanism) and increased reliability.

The drawback that can be derived from system structure is due to the overall cost that requires oversizing the generator so that it can operate above rated speed.

In this paper, the WECS is a direct drive system and includes wind turbine, multi-pole PMSG and buck-to-buck PWM full power converter with buck-boost converter in the DC link. The use of buck-to-buck PWM full power converter insures that the generator currents and the grid currents are sinusoidal. Moreover, the generator side converter is controlled to achieve maximum power extraction. The speed reference which gives maximum power for all wind velocities is evaluated by fuzzy logic algorithm in partial load operation.

When the rated power is reached, active power is limited by adjusting generator speed reference. In this case, rotation speed will exceed the nominal value witch impose a light generator and PWM rectifier oversizing, but the pitch unit is eliminated

and it's possible to associate this electrical control to passive stall control at wind level. The buck-boost converter is used to keep constant the DC voltage upstream grid side converter. In partial load region, the converter operates in boost mode else it operates in buck mode. The grid side converter insures active and reactive power control in order to obtain unitary power factor.

2. Wind turbine modeling

The aerodynamic power converted by the wind turbine is depending on the power coefficient C_p such as:

$$P_T=\frac{1}{2}\rho\pi R^2 C_p(\lambda)V_w^3 \quad (1)$$

where ρ is the air density (ρ=1.225 kg/m^3), *R* is the blade length and V_w is the wind speed.
The power coefficient of the wind turbine depends on tip speed ratio λ, given by:

$$\lambda=\frac{\Omega R}{V_w} \quad (2)$$

where Ω is the rotational speed of the wind turbine and generator.
So, the power coefficient used in wind turbine modeling is expressed as:

$$C_p=\left(\frac{58}{\lambda}-4.53\right)e^{\frac{21}{\lambda}+0.735} \quad (3)$$

Fig. 1. shown the Cp (λ) curve.

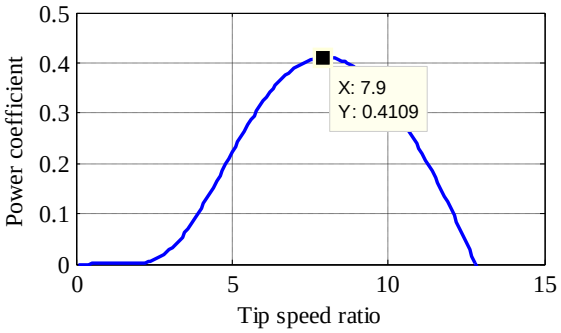

Fig. 1. Power coefficient for the wind turbine model.

2.1. MPPT strategy

Conventionally, to obtain the maximum power from the wind, we use a simple expression based on wind speed measurement, such as:

$$\Omega_{ref}=\frac{\lambda_{opt}V_w}{R} \quad (4)$$

So, the power maximized is given by:

$$P_{max}=\frac{1}{2}\rho C_{p\_max}\frac{\pi R^5}{\lambda_{opt}^3}\Omega_{ref}^3 \quad (5)$$

In this work, we use the fuzzy logic method to obtain the maximum power from the wind. It necessitates only the power and rotational speed measurement of the generator to elaborate the speed reference for generator control. The principal of fuzzy calculus is given in Fig. 2.

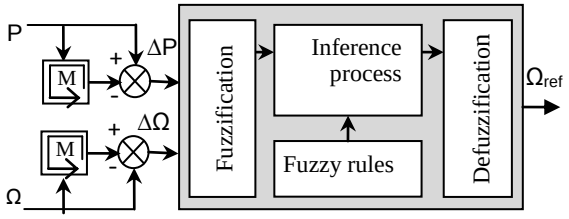

Fig. 2. Fuzzy logic generation of speed reference.

2.1.1. Fuzzification step

The triangular membership functions with overlap used for the input fuzzy sets are shown in Fig. 3. The linguistic variables are presented by NB (Negative Big), NM (Negative Medium), NS (Negative Small), Z (Zero), PS (Positive Small), PM (Positive Medium), and PB (Positive Big).

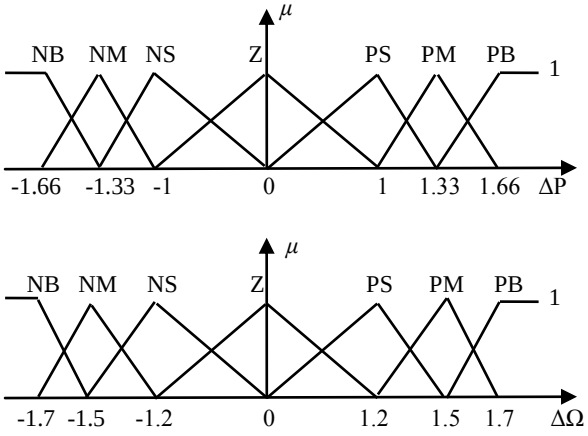

Fig. 3. Fuzzification process.

The grade of input membership functions can be obtained from equation (6) (see Fig. 4).

$$\mu(x)=\max\left(\min\left(\frac{x-x_1}{x_2-x_1},\frac{x_3-x}{x_3-x_2}\right),0\right) \quad (6)$$

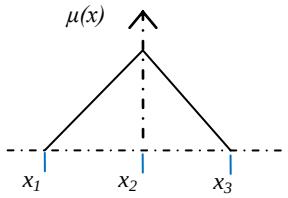

Fig. 4. Grade of membership functions.

2.1.2. Inference process

The fuzzy rules are elaborate according to this instruction:
If « condition 1 » **and** « condition 2 » **then** « conclusion ».
For example, if a big speed augmentation (PB) involves a big power augmentation (PB) then we must increase speed (PB) (Table 1).

Table 1. Fuzzy rules table.

$\Delta\Omega_{k+1}^{ref}$		ΔP						
		GN	**MN**	**PN**	**Z**	**PP**	**MP**	**GP**
ΔΩ	**GN**	GP	GP	MP	Z	MN	GN	GN
	MN	GP	MP	PP	Z	PN	MN	GN
	PN	MP	PP	PP	Z	PN	PN	MN
	Z	GN	MN	PN	Z	PP	MP	GP
	PP	MN	PN	PN	Z	PP	PP	MP
	MP	GN	MN	PN	Z	PP	MP	GP
	GP	GN	GN	MN	Z	MP	GP	GP

2.1.3. Defuzzification step

The defuzzification stage is realized by center of gravity method as schematized in Fig. 5.

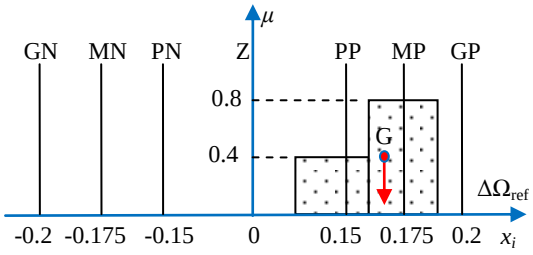

Fig. 5. Defuzzification process.

Such as:

$$\Delta\Omega_{ref(k+1)}=\frac{\sum_{i=1}^{49}(\mu_i\chi_i)}{\sum_{i=1}^{49}\mu_i} \quad (7)$$

where μ_i is the membership grade of the i-th rule and x_i is the coordinate corresponding to the respective output or consequent membership function [22-24].

2.2. Power limitation

For high wind speed the power captured from the wind kinetic energy is limited.

The limitation mode habitually used is the mode (1) as shown in Fig. 6. We kept the power at his nominal value by decreasing power coefficient which corresponds in this case to decreasing tip speed ratio and rotational speed (Pitch regulation).

In this work the power is limited according to second mode: the power coefficient decrease as results of increasing tip speed ratio. In this case the rotational speed can reach his nominal value and the generator torque is controlled in order to kept power constant.

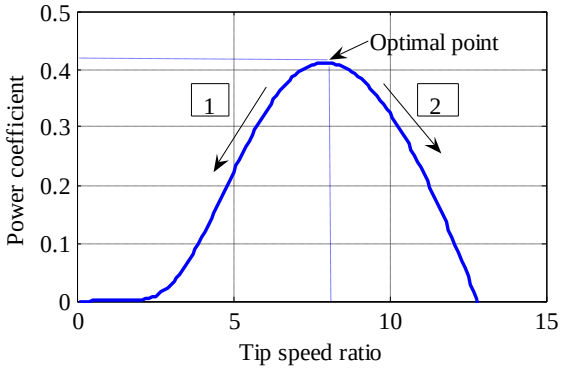

Fig. 6. Power limitation modes.

3. PMSG modeling

The voltage equations of PMSG are expressed as [25]:

$$\begin{cases} v_d=R_s i_d-p\omega\Phi_q+\frac{d}{dt}\Phi_d \\ v_q=R_s i_q+p\omega\Phi_d+\frac{d}{dt}\Phi_q \end{cases} \quad (8)$$

with R_s the stator winding resistance and p is the pair pole number of the synchronous generator.
The direct and quadratic magnetic fluxes are given by (the excitation flux Φ_f is constant)

$$\begin{cases} \Phi_d=L_d i_d+\Phi \\ \Phi_q=L_q i_q \end{cases} \quad (9)$$

with i_d and i_q are, respectively, the direct and quadratic current.
The electromagnetic torque is also expressed as fellow:

$$T_{em}=p\left(\Phi_d i_q-\Phi_q i_d\right) \quad (10)$$

The active and reactive power are given according to

$$\begin{cases} P=v_d i_d+v_f i_q \\ Q=v_d i_q-v_q i_d \end{cases} \quad (11)$$

4. Converters modeling

The basic scheme of electronic converter is given in Fig. 7. Connection functions are defined, for each switch; they represent the ideal commutation and take the value 1 if the switch is close, 0 when he is open.

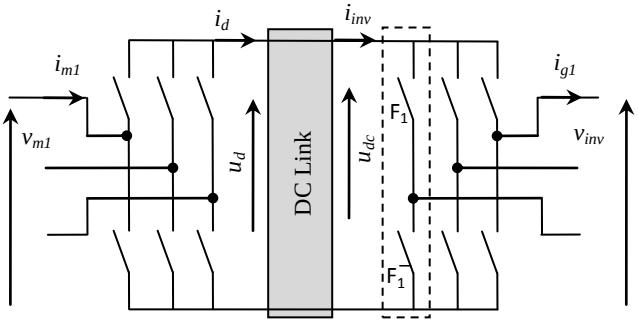

Fig. 7. Electronic converter scheme.

$$F_j=\begin{cases}1 & F_j \text{ is open}\\ 0 & F_j \text{ is close}\end{cases}$$

The rectifier is controlled with a hysteresis PWM, obtained via generator current regulation. The inverter is controlled with natural PWM via grid current regulation.

The DC bus it's a back boost converter controlled through DC voltage regulation.

5. Control system

The global control diagram of the studied system is shown in Fig. 8.

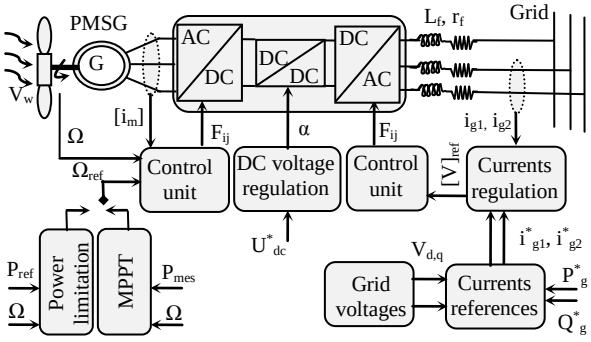

Fig. 8. Global control diagram.

5.1. PMSG Currents Regulation

The hysteresis control of PMSG currents allows keeping the current wave into range defined around the reference value. When current wave reached the band limits, the hysteresis controller generate a logic signal (0 or 1) (Fig. 9). So, for (j=1, 2, 3) we have:

$$\begin{cases}F_j=1 \text{ if } i^*_{mj}-i_{mj}\geq\Delta i\\ F_j=0 \text{ if } i^*_{mj}-i_{mj}\leq\Delta i\end{cases} \quad (12)$$

with Δi is the hysteresis band defined in the controller.

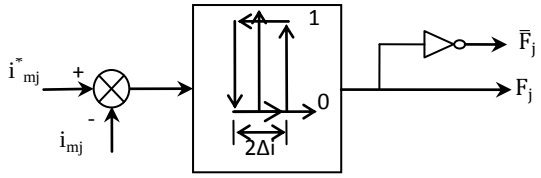

Fig. 9. Hysteresis current regulation.

5.2. DC Bus Regulation

The DC-Bus voltage (grid side) is kept constant at its reference value with help of DC-DC converter (controlled with duty cycle α) through PI regulation. The DC-DC converter is a Buck-Boost ones (Fig.10); it operates on boost mode when the generator speed is under his nominal value and operates in back mode when the generator speed reached his nominal value.

DC voltage and current downstream grid side converter are given by:

$$\begin{cases}u_{dc}=\dfrac{\alpha}{1-\alpha}u_d\\ i_{dc}=\dfrac{1-\alpha}{\alpha}u_d\end{cases} \quad (13)$$

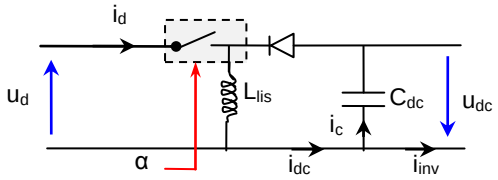

Fig. 10. Buck-Boost converter.

5.3. Grid Currents Regulation

The control of grid side converter has for objective to obtain current and voltage with acceptable wave form and to ensure unitary power factor operation by imposing zero reactive power as reference in the system control.

The electrical equations downstream the converter can be expressed as follows:

$$\begin{cases}I_{g1}=\dfrac{1}{r_f+L_f s}\left(v_{inv1}-v_{g1}\right)\\ I_{g2}=\dfrac{1}{r_f+L_f s}\left(v_{inv2}-v_{g2}\right)\end{cases} \quad (14)$$

The use of mathematical model of converter (with assumption of an equilibrate voltage system) allows expressing simple voltages reference as follows [26]:

$$\begin{pmatrix} v^*_{inv1} \\ v^*_{inv2} \end{pmatrix} = \begin{pmatrix} v^*_{f1} \\ v^*_{f1} \end{pmatrix} + \begin{pmatrix} v_{g1} \\ v_{g2} \end{pmatrix} \quad (15)$$

with PI regulation of grid currents, we obtained the reference voltages v^*_{f1} et v^*_{f2} (Fig. 11), so [26]:

$$\begin{pmatrix} v^*_{f1} \\ v^*_{f2} \end{pmatrix} = PI(s) \begin{pmatrix} i^*_{g1} - i_{g1} \\ i^*_{g1} - i_{g1} \end{pmatrix} \quad (16)$$

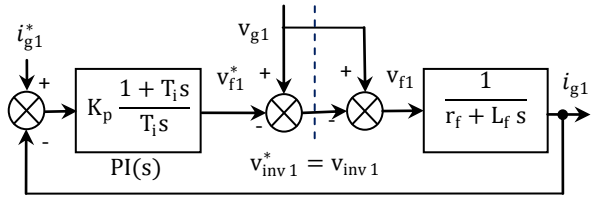

Fig. 11. Grid current regulation.

6. Simulation results and discussion

Numerical simulation of the studied system under Matlab\Simulink® with wind speed profile shown in Figure 12 is realized.

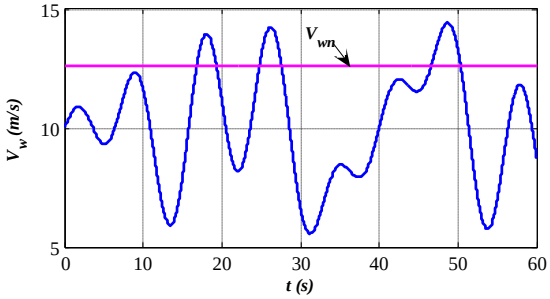

Fig. 12. Random of wind speed.

Rotation speed curves are given in Fig. 13 (with Ω_n nominal speed, Ω_g generator speed, Ω_{opt} optimal speed and Ω_{LF} fuzzy logic calculated speed). The fuzzy logic calculated speed reference coincides with the optimal ones, which gives optimal value of power (Fig. 14).

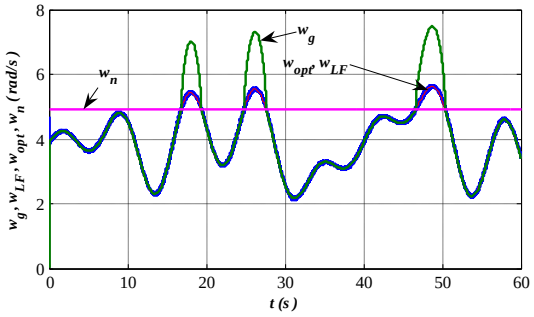

Fig. 13. Rotation speed curves.

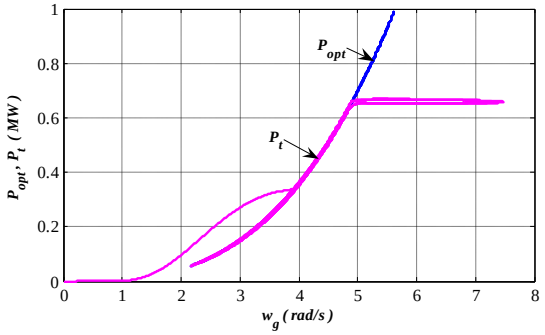

Fig. 14. Optimal and real power.

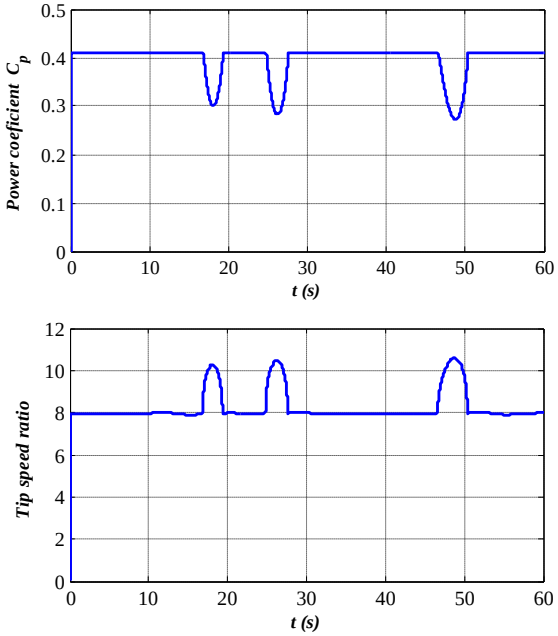

Fig. 15. Power coefficient and tip speed ratio.

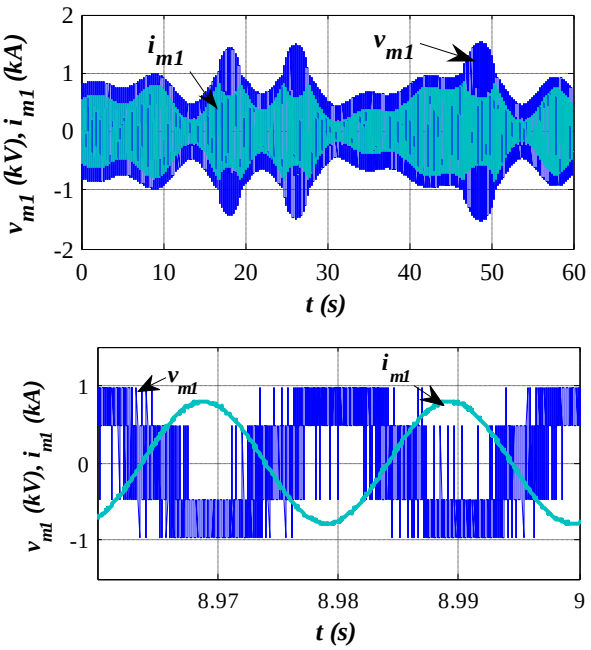

Fig. 16. PMSG voltage and current.

Over nominal operation point, the nominal rotation speed is reached, but the power captured from the wind is limited at the nominal value. The corresponding power coefficient and tip speed ratio for those two operation cases are shown in Fig. 15.

Fig. 16. gives PMSG voltage and current wave form and Fig. 17 presented active and reactive power and eventually power factor. When the nominal operation point is reached, the reactive power decrease; which contribute to improve power factor.

DC voltage and current are shown in Fig. 18 and Fig. 19 respectively. As we can remark, DC voltage downstream grid side converter is practically constant.

Fig. 20. gives grid voltage and current with sinusoidal wave form at constant frequency. Active and reactive powers are given in Fig. 21, reactive power is practically equal to zero which gives unitary power factor for grid connection (Fig. 22).

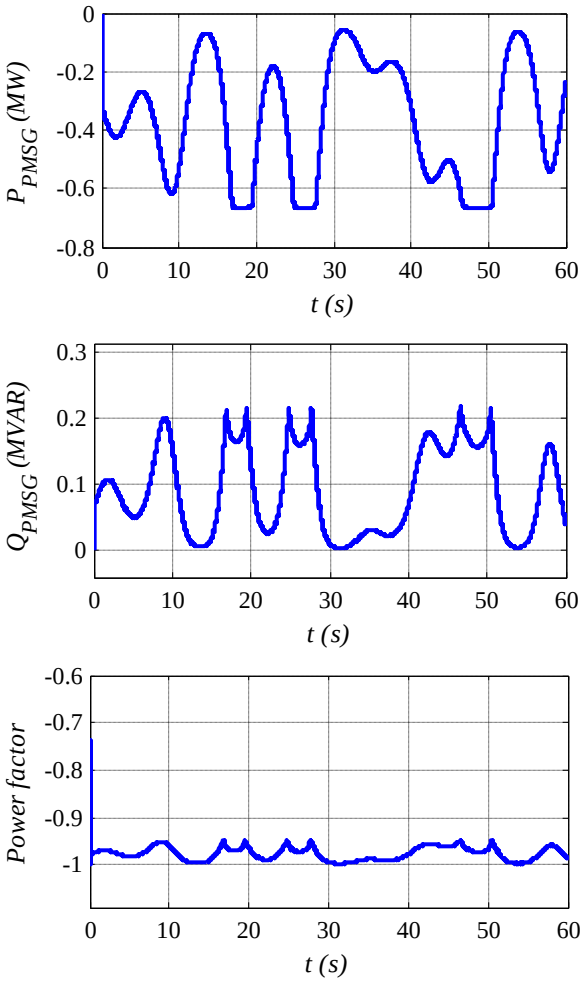

Fig. 17. PMSG active and reactive power and power factor.

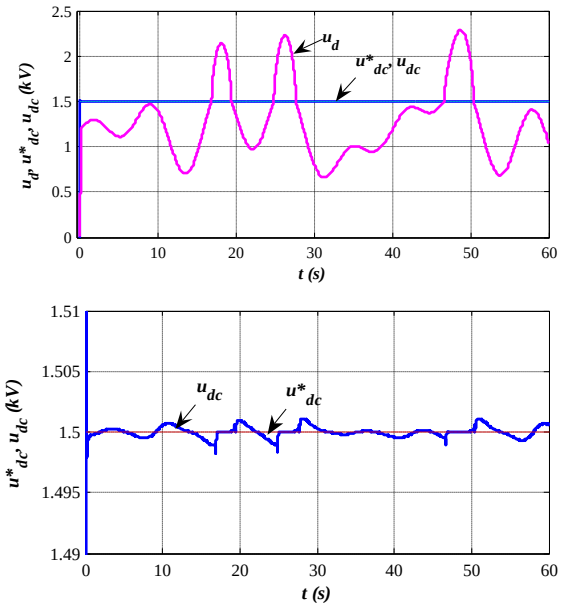

Fig. 18. DC voltages.

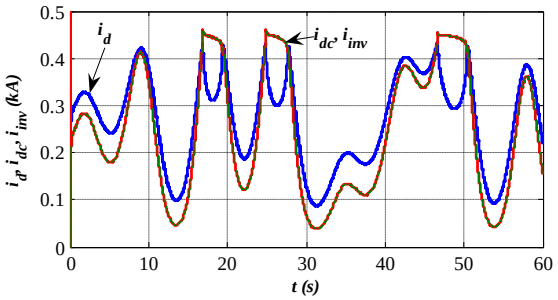

Fig. 19. DC currents.

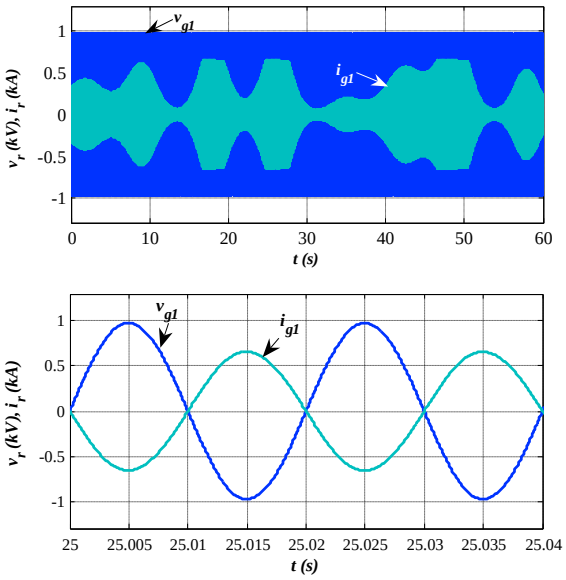

Fig. 20. Grid voltage and current.

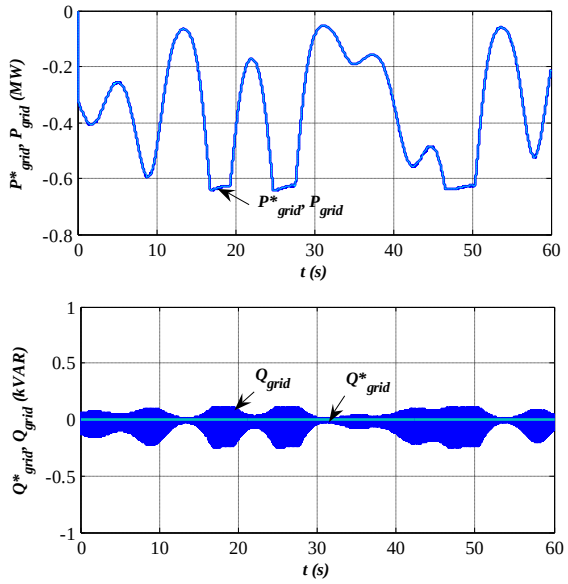

Fig. 21. Grid active and reactive power.

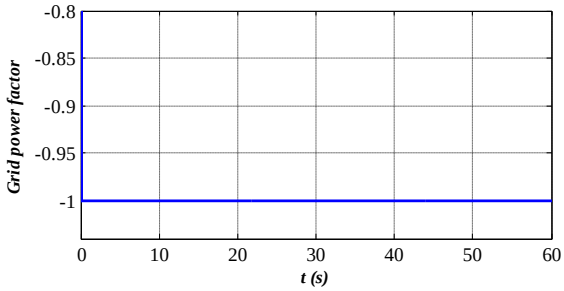

Fig. 22. Grid power factor.

7. Conclusion

Significant improvements are introduced in WECS by transition from fixed speed to variable speed operation. However, control system for variable and low speed generator should continue to increase effectiveness and efficiency of innovative control system.

A control of wind conversion system based on direct drive PMSG has been developed and both MPPT operation and power limitation are considered in this work. Simulation results with Matlab\Simulink software environment prove the effectiveness of fuzzy logic control to track and extract maximum power to grid. Fuzzy logic control allows overcoming problems linked to the inaccuracy of measuring wind speed and to the effect of system parameters variation with time and varied environment.

Over the nominal operation point, the power captured from wind's kinetic energy has been limited by means of generator torque control. As results, generator rotation speed and voltage will reach nominal values that should take into account in generator design and electronic device but considerable simplifications of the mechanical turbine system are obtained by omitting mechanicals unit.

Appendix

The principal parameters of the studied system are given below.

Wind turbine: R=20.41 m, blade number =3

PMSG: R_s= 0.01 Ω, L_d=L_q =0.001 H, p=64,

Φ_f=2.57 Wb, J=3800 Kg.m^3, f= 26.75N.m.s/rad.

DC-link: U_{dc}=1.5 kV, C_{dc}=0.015 F.

Filter: L_f=0.001 H, r_f=0.01 Ω

Electrical grid: f=50 Hz, V_n=690 V.

References

1. Baroudi J.A., Dinavahi V., Knight A.M.: *A review of power converter topologies for wind generators.* In: Renewable Energy, 32 (2007), p. 2369-2385.
2. Hansen L.H.: *Generators and power electronics technology for wind turbines*. In: The 27th Annual Conference of the IEEE Industrial Electronics Society IECO'01, 2001, p. 2000-2005.
3. Laverdure N. : *Sur l'intégration des générateurs éoliens dans les réseaux faibles ou insulaires (On the integration of wind generator in low or island grid)*. Thèse de Doctorat, 2005, INPG, France.
4. Aouzellag D., Ghedamsi K., Berkouk E.M.: *Network power flux control of a wind generator*. In: Renewable Energy, 34 (2009), p. 615-622.
5. Sánchez J.A., Veganzones C., Martinez S., Blazquez F., Herrero N., Wilhelmi J.R.: *Dynamic model of wind energy conversion systems with variables speed synchronous generator and full-size power converter for large-scale power system stability studies*. In: Renewable Energy, 33 (2008), p. 1186-1198.
6. Wua F., Zhang X.P., Ju P.: *Small signal stability analysis and control of the wind turbine with the direct-drive permanent magnet generator integrated to the grid*. In: Electrical Power System Research, 79 (2009), p. 1661-1667.
7. Li H., Chen Z.: *Design optimization and site matching of direct-drive permanent magnet wind power generator systems*. In: Renewable Energy, 34 (2009), p. 1175-1184.
8. Whei-Min L., Chih-Ming H., Fu-Sheng C.: *Design of intelligent controllers for wind generation system with sensorless maximum wind energy control*. In: Energy Conversion and Management, 52 (2011), p. 1086-1096.
9. Muljadi E.: *Pitch-controlled variable-speed wind turbine generation*. In: IEEE Transactions on Industry Applications, 37 (2001), p. 240-246.
10. Jauch C., Islam S.M., Sørensen P., Jensen B.B.: *Design of a wind Turbine pitch angle controller for*

power system stabilization. In: Renewable Energy, 32 (2007), p. 2334–2349.
11. Junsong W., Norman T., Zhiwei G.: *Synthesis on PI-based pitch controller of large wind turbines generator*. In: Energy Conversion and Management, 52 (2011), p. 1288-1294.
12. Albadi M.H., El-Saadany E.F.: *New method for estimating CF of pitch-regulated wind turbines.* In: Electrical Power System Research, 80 (2010), p. 1182-1288.
13. Whei-Min L., Chih-Ming H., Ting-Chia O., Tai-Ming C.: *Hybrid intelligent control of PMSG wind generation system using pitch angle*. In: Energy Conversion and Management, 52 (2011), p. 1244-1251.
14. Melício R., Mendes V.M.F., Catalão J.P.S.: *Transient analysis of variable-speed wind turbines at wind speed disturbances and a pitch control malfunction*, In: Applied Energy, 88 (2011), p. 1322-1330.
15. Broe A.M., Drouilhet S., Gevorgian V.: *A peak power tracker for small wind turbines in battery charging applications.* In: IEEE Transactions on Energy Conversion, 14 (1999), p. 1630-1635.
16. Calderaro V., Galdi V., Piccolo A., Siano P.: *A fuzzy controller for maximum energy extraction from variable speed wind power generation systems*. In: Electrical Power System Research, 78 (2011), p. 1109-1118.
17. Munteanu I., Antoneta I.B., Ceanga E.: *Wind turbulence used as searching signal for MPPT in variable-speed wind energy conversion systems.* In: Renewable Energy, 34 (2009), p. 322-327.
18. Munteanu I., Bratcu A.I., Cutululis A.A., Ceanga E.: *Optimal control of wind energy conversion system.* Springer-Verlag, London, 2008.
19. Senjyu T., Ochi Y., Kikunaga Y., Tokudome M., Yona A., Muhando E.B., Urasaki N., Funabashi T.: *Sensor-less maximum power point tracking control for wind generation system with squirrel cage induction generator.* In: Renewable Energy, 34 (2009), p. 994-999.
20. Ying-Yi H., Shiue-Der L., Ching-Sheng C.: *MPPT for PM Wind Generator using Gradient Approximation*. In: Energy Conversion and Management, 50 (2009), p. 82-89.
21. Carranza O., Figueres E., Garcerá G., Gonzalez L.G. : *Comparative study of speed estimators with highly noisy measurement signals for wind energy generation systems*. In: Applied Energy, 88 (2011), p. 805-813.
22. Muyeen S.M., Tamura J., Murata T.: *Stability augmentation of a grid-connected wind farm.* Springer-Verlag, London, 2009.
23. Altas I.H., Sharaf A.M.: *A Novel maximum power fuzzy logic controller for photovoltaic solar energy systems*. In: Renewable Energy, 33 (2008), p. 388-399.
24. Bia Y., Zhuang H., Wang D.: *Advanced fuzzy logic technologies in industrial applications.* Springer-Verlag, London, 2006.
25. Jean Paul L., Claude B. : *Commande numérique des machines synchrones (Digital control of synchronous machines).* Techniques d'Ingénieur (1999), Référence D3644.
26. Hamrouni N., Jraidi M., chérif A. : *New control strategy for 2-stage grid-connected photovoltaic system.* In: Renewable Energy, 33 (2008), p. 2212-2221.